Supporting information

Structural Design of Oxygen Reduction Redox Mediators (ORRMs) Based on Anthraquinone (AQ) for the Li-O_2 battery

Xiang-Bin Han and Shen Ye*

Department of Chemistry, Graduate School of Science, Tohoku University, Sendai, 980-8577, Japan.

Corresponding Author *Email for Shen Ye: ye.shen@tohoku.ac.jp

Experimental details

Materials

Oxygen and Argon gas were used directly from the gas company without special treatment with a dew point temperature of −75°C (water: 1.204 ppm) according to the factory test result. Two oxygen gloveboxes (Unico, Japan) were used, and one of them equipped with a water removal system that can keep water content at 0.2 ppm, another just filling oxygen gas without any water removal system (RH: 5−6%, 1200−1500 ppm). Water and oxygen in Ar glovebox are < 1 ppm and < 10 ppm, respectively.

6,13-pentacenequinone (PQ), 5,12-naphthacenequinone (NAQ), anthraquinone (AQ), 1-nitroanthraquinone (MNAQ), 1-chloroanthraquinone (MClAQ) and 1,5-dichloroanthraquinone (DClAQ) were obtained from Tokyo Chemical Industry Co., Ltd.. 1,5-Dinitroanthraquinone (1,5-DNAQ) and 1,8-dinitroanthraquinone (1,8-DNAQ) were obtained from Aldrich. 1-Cyanoanthraquinone (MCAQ) and 1,5-dicyanoanthraquinone (DCAQ) were synthesized and characterized by ourselves, and the detailed process was shown in the following section. The lithium iron phosphate used in the experiment was purchased from Hohsen Corp., Japan. All the reagents were stored in the Ar atmosphere glovebox (Lab Star).

Water control procedures

TEGDME solvent was purified via distillation by the Schlenk tube technique (Fig. S1) because the solvent purity will affect the battery performance.[1]

Remove the kerosene on the sodium metal surface with paper and cut it into small pieces for use. Sodium (1.5 g) and 9 g of benzophenone were put in a 1000 mL flask containing 500 mL TEGDME. All of this process was finished in the Ar glove box to avoid sodium exposure to water and oxygen. Then take the flask out of the glovebox and connect to the distillation system, vacuum the system, and increase the temperature of the oil bath. Please note, the temperature setting is increased by 10℃ during the initial heating process, and the increment is adjusted to 2℃ when it approaches the boiling point. The final boiling temperature depends on the vacuum degree of the distillation system. Adjust the stirring speed to control the collection rate of the distillate to one to two drops per second. After the distillation fills in dried Ar into the Schlenk flask contains TEGDME and disassembles it from the distillation system under continuous Ar gas flow and seal it by glass stopper. Then transfer the flask to the Ar glove box. Please note that more moderate water scavenger calcium hydride can also be used in this step.

Fig. S1 Schlenk tube system for distillation.

The water content has a noticeable decrease, but not less than 10 ppm, it is about 30 ppm. The active molecular sieves further dried the distillate for three to four days — finally, the water content below 10 ppm. The water content measured by Karl Fischer Moisture Titrator (MKC-710, Kyoto Electronics Manufacturing Co., Ltd.). All the results were the average value of three times of measurement values.

Molecular sieves activation procedure

Molecular sieves were firstly washed by acetone and dried to remove the solvent, then put them in oven-dried at 500℃ for 12 h, then transfer to a Schlenk flask further dried under vacuum at 180℃ for 12 h. After drying, filling Ar in the flask to balance the pressure and transferring it to the Ar glove box.

Battery test and characterization

Cyclic voltammetry measurements were carried out by Potentiostat/Galvanostat 2020 (TOHO Technical Research). A three-electrode system is used in an H type glass tube with a glassy carbon as a working electrode and Li metal as counter and reference. Discharge curves were measured by the Neware battery test system (5V−50 mA, Neware Technology Limited Shenzhen, China). 4 mL 0.5 M LiTFSI-TEGDME solution in an H type glass tube cell was used in the CVs experiments. For the coin cell test, 0.1 mL 0.5 M LiTFSI-TEGDME solution was used as the electrolyte solution.

Fig. S2 Coin cell structure.

The Hitachi SU-70 Analytical Field Emission Scanning Electron Microscope (SEM) was used to observe the surface morphologies of carbon paper and discharge product lithium peroxide. After discharge, the cell was disassembled in the Ar glove box. Firstly, remove the electrolyte solution in the cathode (carbon paper) by Kimwiper, and then wash with a little DME and remove solvent with Kimwiper, repeat this procedure for three times. All the washed cathode was then transferred into the Schlenk flask and dried under vacuum. After drying, the Schlenk flask was filled in dry Ar and then moved them to the Ar glove box before the SEM test. During the SEM measurement, prepare the sample as soon as possible to avoid the carbon paper contact with air for a long time.

Raman Spectroscopy of discharge electrodes was measured by Horiba XploRA plus Raman microscope with LabSpec6 workstation under 10 mW laser power at 532 nm. In situ SERS experiment, Excitation light of 785 nm laser was used. The attenuated total reflection FTIR spectroscopy (ATR−FTIR) was carried out by Spectrum Two (Perkin Elmer) with a universal ATR accessory (diamond prism, single reflection) in an Ar-filled glovebox. Powder X-ray diffraction (PXRD) was conducted by BrukerAX D8Discovery-TM, and the electrode was wrapped on both sides with a Kapton film.

Ultraviolet−visible titration (UV−vis) was measured with UV−vis spectrometer Lambda 650 (PerkinElmer). The $TiOSO_4$ titration method is similar to many reported papers.[2-3] The discharged batteries were disassembled in the Ar glovebox and remove the electrolyte solution in cathode and separator with Kimwiper as much as possible and put them into a small sample bottle. Add a certain amount of water to the bottle (depends on discharge capacity) and add a certain amount of (15% wt) $TiOSO_4$ (also depends on the capacity, usually 110−120% to the capacity). We use the molar extinction coefficient of TiO_2^{2+} (679.5 ± 20.8 L mol^{-1} cm^{-1}) to calculate the yield of Li_2O_2 due to the inaccurate purity of commercial Li_2O_2.[4]

Calculation of water content in the electrolyte after discharge

A unique method was designed to calculate the water content in the electrolyte solution after discharge.

Firstly, disassemble the coin cells and pick up the separator, then put them in a small glass vial. Usually, at least 4 pieces or more of separators were used because each piece soaks a little electrolyte solution (60-80 mg).

Secondly, add some fresh TEGDME solvent (m_2) contains a certain water content ($A1$).

Thirdly, keep the mixture solution in the glovebox for 10 h.

Last, measure the water content of the mixed solution ($A2$) by Karl Fischer titrator.

The water content in the final electrolyte was set as x ppm, and the following equation was used to calculate the water content in the electrolyte after discharge.

$$m_1 \div 10^3 \times \frac{x}{10^6} + m_2 \div 10^3 \times \frac{A1}{10^6} = (m_1 \div 10^3 + m_2 \div 10^3) \times \frac{A2}{10^6} \qquad x = ?\ \text{Ppm}$$

Setting: unit of m is g, and for A and x is ppm

m_1: the weight of electrolyte soaked in separators, x: water content in them;

m_2: the weight of added fresh TEGDME, $A1$: water content in it; please note that $A1$ should be larger than 10 ppm because small $A1$ always causes a significant deviation.

Table S1 Water content after discharge showed in the following table, t means the time of battery stays in the corresponding atmosphere, including discharge time and shelving time on purpose.

H_2O in O_2	RH 5-6%	RH 5-6%	RH 5-6%	RH 5-6%	0.2ppm
m: (separators+ electrolyte)	0.4748	0.6275	0.3014	0.5607	0.321
m: (separators)	0.0642	0.0856	0.0428	0.0855	0.0428
electrolyte: m_1	0.4106	0.5419	0.2586	0.4752	0.2782
TEGDME: m_2	4.1873	4.0684	4.075	4.0526	4.028
H_2O in TEGDME:A1/ppm	33.40675	33.40675	33.40675	33.40675	33.40675
H_2O in mixture: A2/ppm	65.1224	80.028	73.7193	185.8748	33.7891
x/ppm	**388.5**	**430.0**	**708.9**	**1486.1**	**39.3**
time/h	17	25	48	79	148
average speed: ppm/h	**22.3**	**16.8**	**14.6**	**18.7**	**0.2**

The rate of water increase varies from 14.6 to 22.3 ppm/h in high water content oxygen because of the humidity change day by day within a range (RH: 5−6%, 1200 −1500 ppm). While for the controlled ones after discharge and keep in the glovebox for a long time, the water content just has a slight increase but still less than 40 ppm.

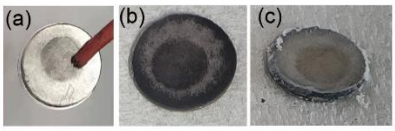

Fig. S3 Li metal anode after discharge under different oxygen environments, the circular shadow in the center of the Li anode corresponds to the size of carbon cathode. (a) The lithium metal discharged in low water content oxygen glovebox (0.2 ppm) keeps metallic luster. The lithium metal discharged in high water content oxygen glovebox becomes black (b) due to reacting with water and further change to white LiOH (c). The discharge time of Li metal in (c) is longer than (b).

Synthesis and characterization of DCAQ and MCAQ

DCAQ: 1,5-dichloroanthraquinone (1.0 g, 3.6 mmol) and Cu(I)CN (1 g, 11 mmol) were dispersed in *n*-methyl pyrrolidinone (NMP) (50 mL) and heated to 180℃ under argon for 6 hours. The hot dark brown solution was poured onto ice (300 g), and the brown precipitate was filtered, washed with water and dried under vacuum. The precipitate was decomposed with 4 M nitric acid (100 mL) at 60℃ for 4 hours. The resulting brown solid was filtered, washed with water and dried, and then recrystallized with phenylacetonitrile, obtaining brown needle crystals of 1,5-dicyanoanthraquinone (DCAQ) (0.64 g, 67 %). Mass spectroscopy was used to confirm the molecular weight (Fig. S4). MS (EI) m/z: 281 (DCAQ+Na 100%). Elemental analysis (EA) : calc.: C: 74.42 %, H: 2.34 %, N: 10.85; exp.: 74.390 %, H: 2.362 %, N: 10.689 %.

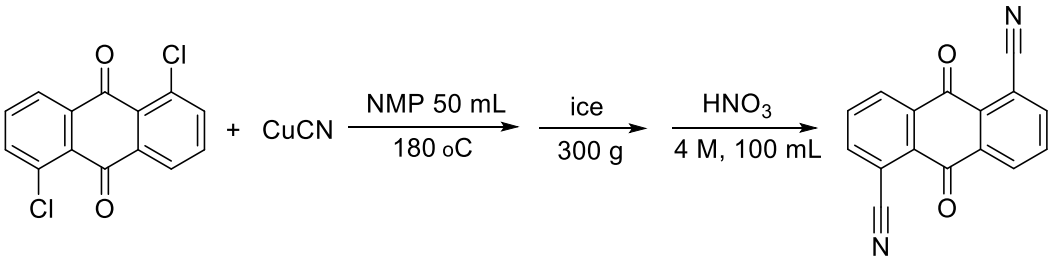

Scheme S1 Synthesis procedures of DCAQ.

MCAQ: 1-chloroanthraquinone (1.0 g, 4.1 mmol) and Cu(I)CN (0.51 g, 5.7 mmol) were dispersed in n-methyl pyrrolidinone (NMP) (50 mL) and heated to 180℃ under argon for 6 hours. The hot dark brown solution was poured onto ice (300 g), and the brown precipitate was filtered, washed with water and dried under vacuum. The precipitate was decomposed with 4 M nitric acid (100 mL) at 60℃ for 4 hours. The resulting brown solid was filtered, washed with water and dried, and then recrystallized with phenylacetonitrile, obtaining light brown needle crystals of 1-cyanoanthraquinone (MCAQ) (0.54 g, 56 %). Mass spectroscopy was used to confirm the molecular weight (Fig. S5). MS (EI) m/z: 256 (MCAQ+Na 100 %). EA : calc.: C: 77.25 %, H: 3.03 %, N: 6.01%; exp.: 77.322 %, H: 3.022 %, N: 5.999 %.

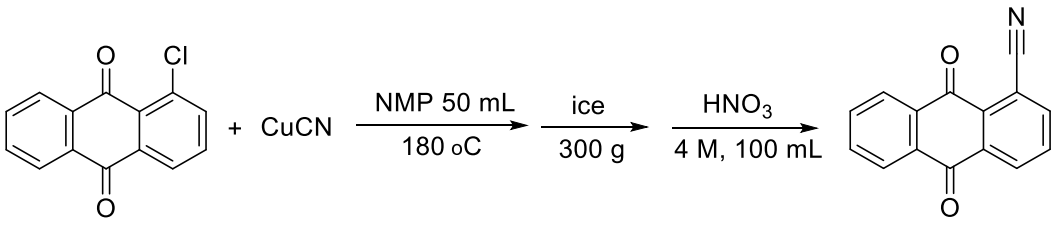

Scheme S2 Synthesis procedures of MCAQ.

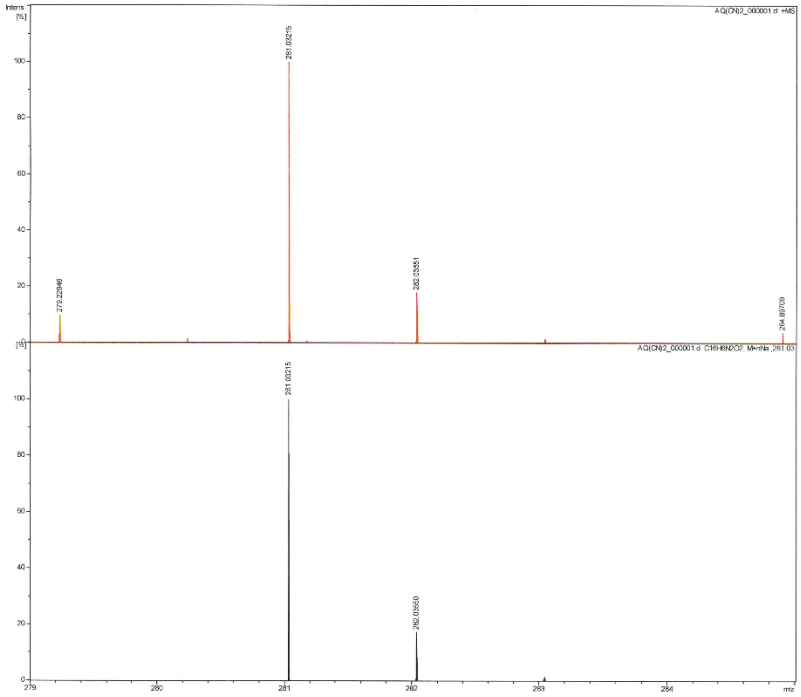

Fig. S4 Mass spectroscopy results for compound DCAQ.

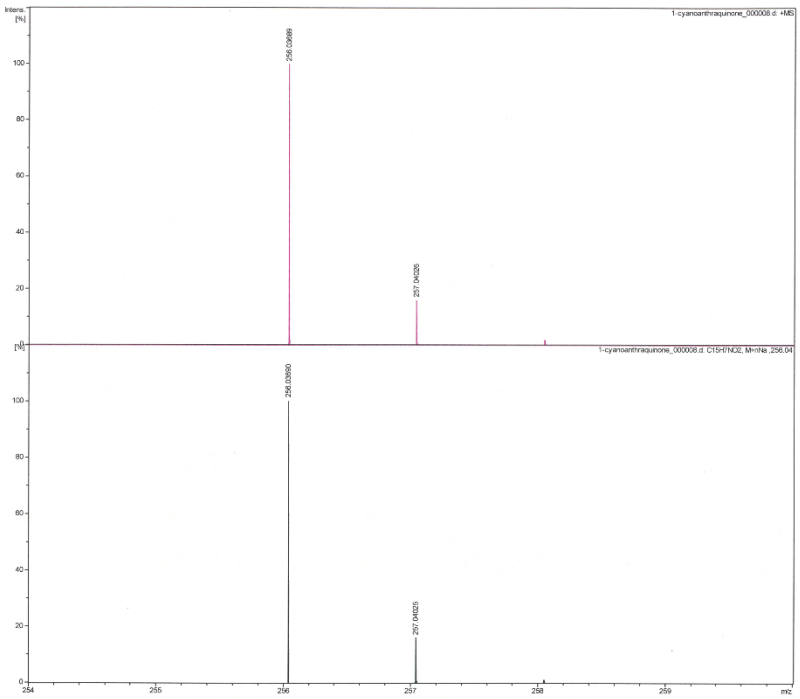

Fig. S5 Mass spectroscopy results for compound MCAQ.

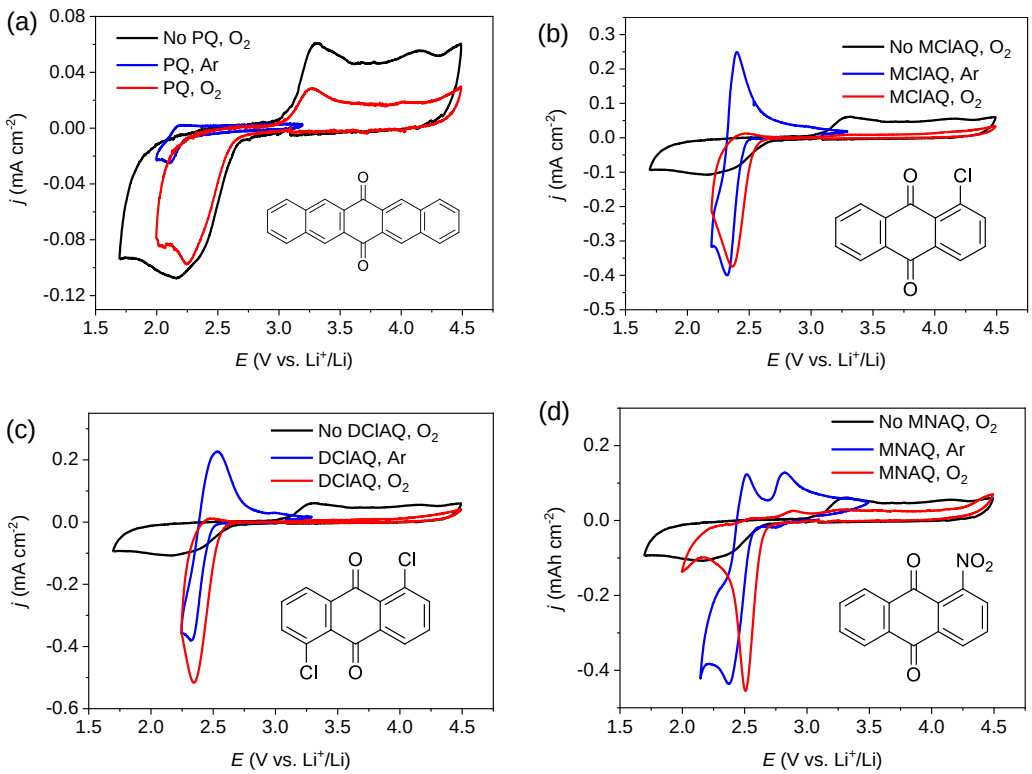

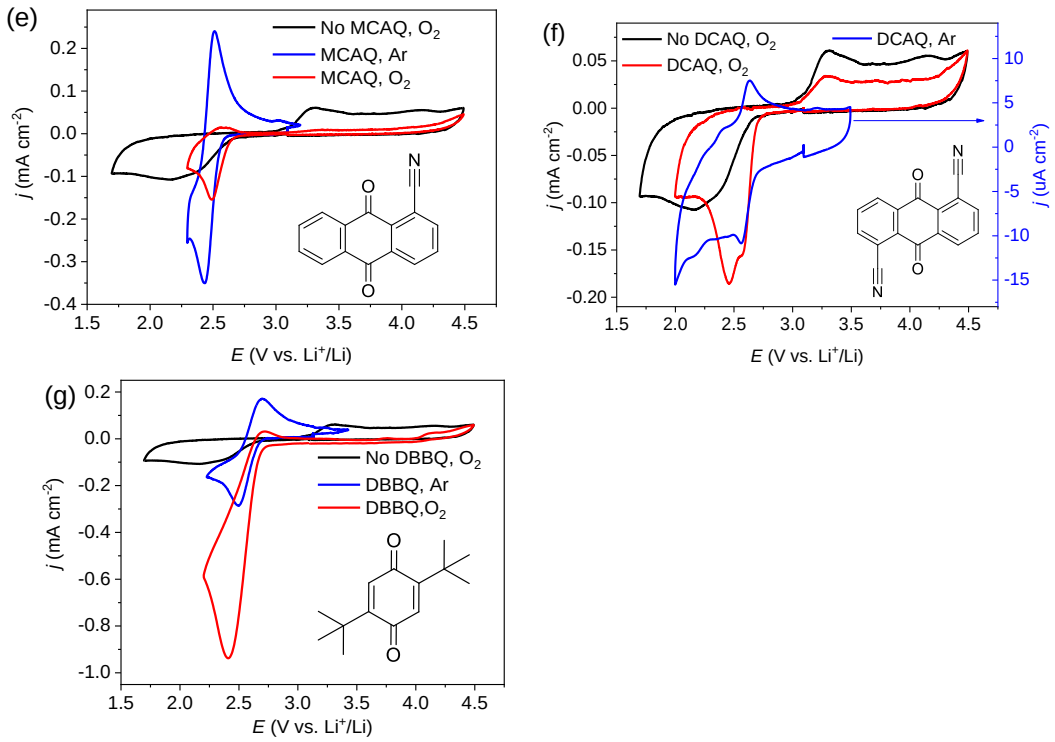

Fig. S6 Cyclic voltammograms of remaining AQ derivatives in 0.5 M LiTFSI inTEGDME under Ar (blue), O_2 (red) and pure O_2 (black) reduction on glassy carbon electrode with a scan rate of 10 mV s^{-1}. (a) PQ (s); (b) MClAQ (10mM); (c) DClAQ (s); (d) MNAQ (10 mM); (e) MCAQ (10 mM); (f) DCAQ (s); (g) DBBQ (10 mM). Notably, s means the saturated solution (less 5 mM) was used for these compounds.

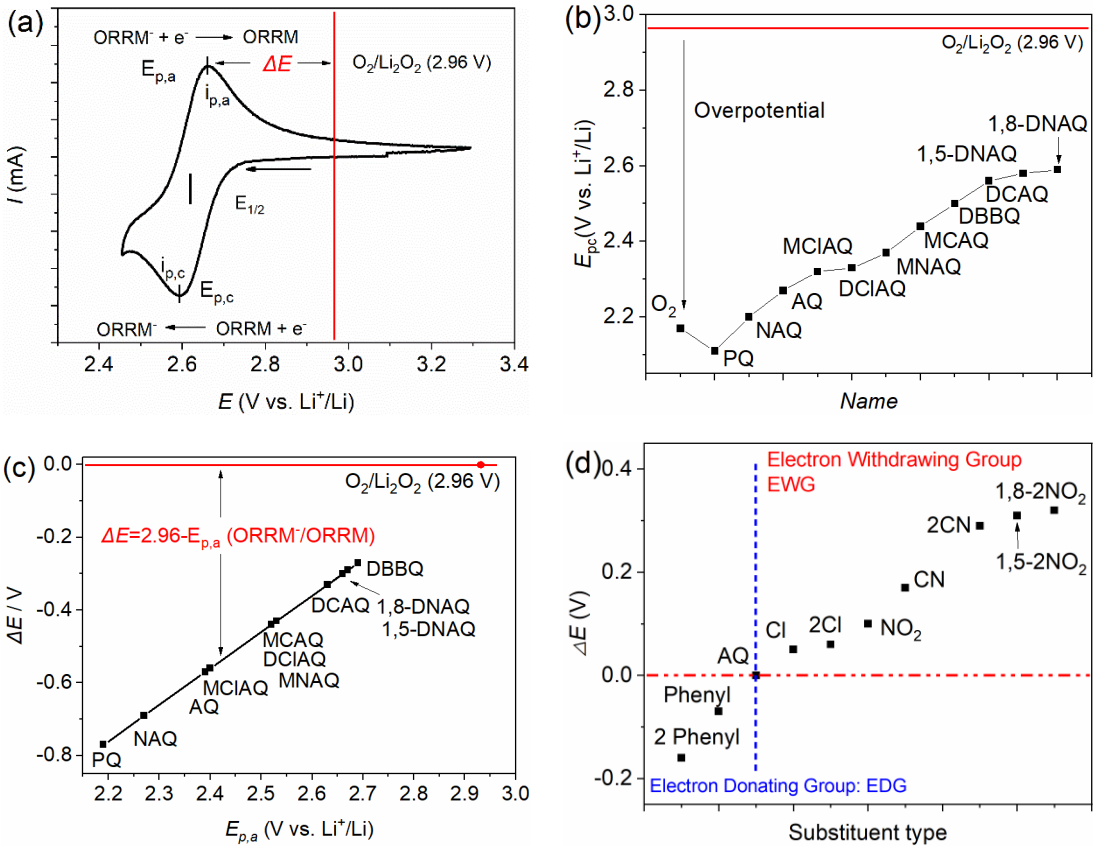

Fig. S7 (a) The scheme of $E_{p,c}$, $E_{p,a}$, of ORRM, and E_{eq} of O_2/Li_2O_2. (b) The overpotential of Li-O_2 battery on the discharge. The squares in the curve are the $E_{p,c}$ value of ORRMs, and oxygen. When the ORRM is employed, the discharge plateau of ORRM replaces the electrochemical oxygen reduction potential plateau. As shown in Fig. S7b, the $E_{p,c}$ of ORRM is higher than the actual $E_{p,c}$ of oxygen. Therefore, the battery discharge plateau is close to the theoretical value 2.96 and decrease the discharge overpotential for Li-O_2 battery containing ORRM with positive $E_{p,c}$ value. That's why this paper design the AQ structure and move the $E_{p,c}$ close to 2.96 V. (c) The potential difference (ΔE) between the equilibrium potential of Li-O_2 battery and the $E_{p,a}$ of ORRM. The reaction of $ORRM^-$ and O_2 is the essential step for ORRM in the whole catalytic process. Generally, the ΔE determines the reaction rate of $2ORRM^- + O_2 + 2Li^+ \rightarrow Li_2O_2 + 2ORRM$. Therefore, we find the PQ has the biggest ΔE, which means the PQ^- would react O_2 fast than $DNAQ^-$. However, the DNAQ has better performance than PQ as ORRM, and even the ΔE is smaller than PQ. Because DNAQ has higher than $E_{p,c}$ than PQ, therefore, there is no competition reaction between electrochemical DNAQ reduction and electrochemical O_2 reduction. Electrochemical O_2 reduction, the key reason for the small discharge capacity of Li-O_2 battery, is avoided in the presence of DNAQ, and large discharge capacity is obtained. In conclusion, we need a balance between the $E_{p,c}$ (high discharge plateau), and $E_{p,a}$ (reaction rate between $ORRM^-$ and O_2) in the selection of ORRMs. Therefore, we found 1,5-DNAQ is the best ORRM in this AQ derivatives series even its solubility is not as well as 1,8-DNAQ. (d) $\Delta E_{p,c}$ between AQ and its derivatives. The $E_{p,c}$ of AQ, was set as the zero points. It shows the contribution of the amount of substitute group, type, and position to the $E_{p,c}$ of AQs. The detailed data in Fig. S7 is shown in Table S1.

Table S1 The reduction ($E_{p,c}$) and oxidation peak potential ($E_{p,a}$) of ORRMs under Ar collected from CV curves were summarized in the first two rows. $E_{1/2}$ is the average value of $E_{p,c,}$ and $E_{p.a}$. ΔE is the potential difference between the equilibrium potential of Li-O_2 battery and the $E_{p,a}$ of ORRM. ΔV is $E_{p,c}$ difference of AQ and its derivatives.

	O_2	PQ	NAQ	AQ	MClAQ	DClAQ	MNAQ	MCAQ	DBBQ	DCAQ	1,5-DNAQ	1,8-DNAQ
$E_{p,c}$	2.17	2.11	2.20	2.27	2.32	2.33	2.37	2.44	2.49	2.56	2.58	2.59
$E_{p,a}$	-	2.19	2.27	2.39	2.40	2.53	2.52	2.52	2.69	2.63	2.67	2.66
$E_{1/2}$	-	2.15	2.235	2.33	2.36	2.43	2.445	2.48	2.60	2.595	2.625	2.625
ΔE		0.77	0.69	0.57	0.56	0.43	0.44	0.44	0.27	0.33	0.29	0.3
Group	-	2 Phenyl	Phenyl	-	1 Cl	2 Cl	NO_2	CN	-	2 CN	2 NO_2	2 NO_2
ΔV	-	-0.16	-0.07	0	0.05	0.06	0.1	0.17	0.22	0.29	0.31	0.32

Table S2 Discharge capacity of Li-O_2 batteries with DBBQ and 1,8-DNAQ under different concentrations. The cut-off voltage is 2.4 V.

S (cm^2)	c (mM)	DBBQ (mAh cm^{-2})	1,8-DNAQ (mAh cm^{-2})
0.5	10	1.02±0.01	0.96±0.04
0.5	20	2.11±0.04	2.17±0.01
0.1256	20	4.78±0.27	4.51±0.47

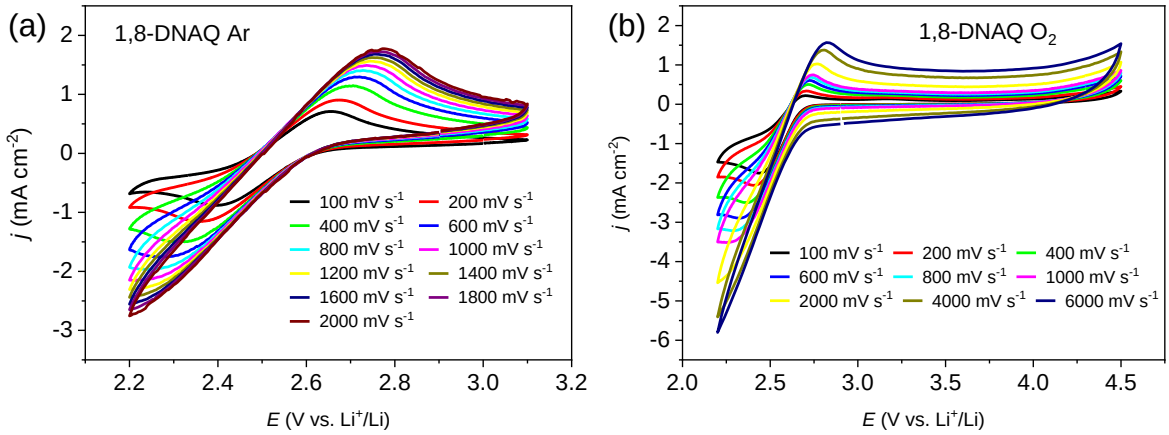

Fig. S8 Reaction kinetics of ORRM. CVs of 10 mM 1,8-DNAQ under Ar (a) and O_2 (b) with various scan rates. With the scan rate increase, the anodic peak also increases under the oxygen saturated state. It means the 1,8-DNAQ$^-$ is oxidized to 1,8-DNAQ, which supports the conclusion that the chemical reaction rate between ORRM$^-$ and oxygen is slow than the electrochemical reaction of ORRM to ORRM$^-$. As for the slow reaction kinetics between ORRM$^-$ and oxygen, a high concentration of ORRM was used in the coin cell discharge process. Fig. S9 shows the higher concentration results in high discharge capacity.

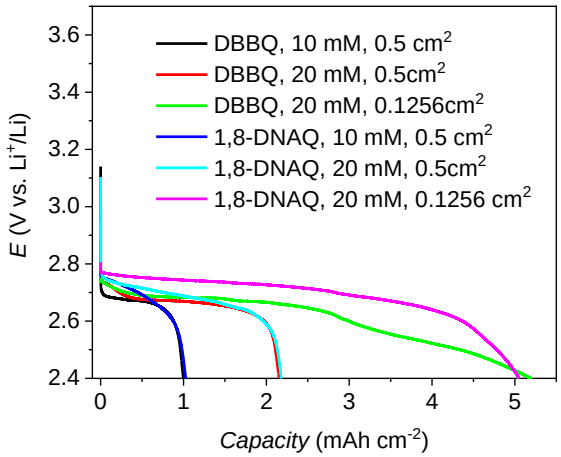

Fig. S9 The concentration effect of ORRM. Li-O_2 batteries discharged with DBBQ and 1,8-DNAQ under different concentrations and electrode areas. In this part, the diameter of the electrode is 8 mm for 0.5 cm^2 and 4 mm for 0.13 cm^2. Please note that the concentration of 1,8-DNAQ can not go up to 40 mM. Therefore, the smaller size of the electrode was used to improve the concentration of 1,8-DNAQ on a unit area. The reduction peak of AQ has a significant overlap area with oxygen reduction. Therefore, there has surface Li_2O_2 growth, the concentration effect would be affected by the surface oxygen reduction, and we supply for the discharge capacity result of 1,8-DNAQ to investigate the concentration effect of ORRMs as a supplement for Figure 2.

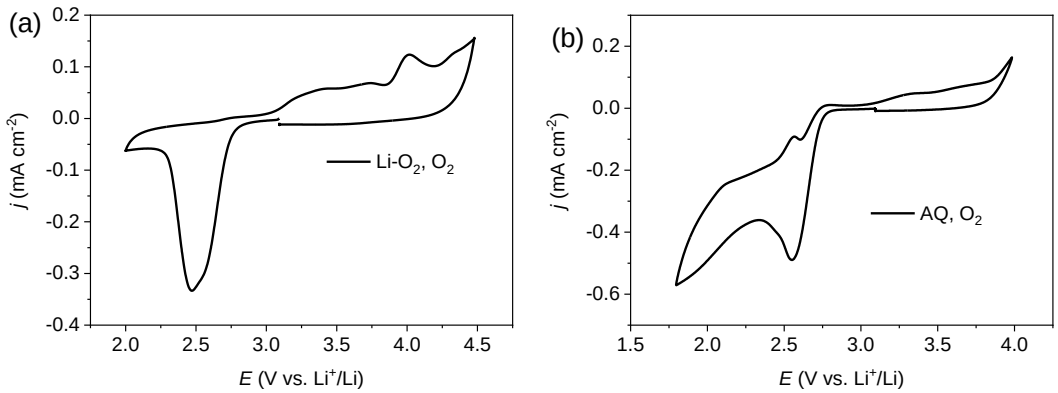

Fig. S10 Cyclic voltammograms observed in (a) 0.1 M $LiClO_4$-DMSO and (b) 0.1 M $LiClO_4$-DMSO with 10 mM AQ. All solutions were saturated by O_2. Supplement for Fig. 4.

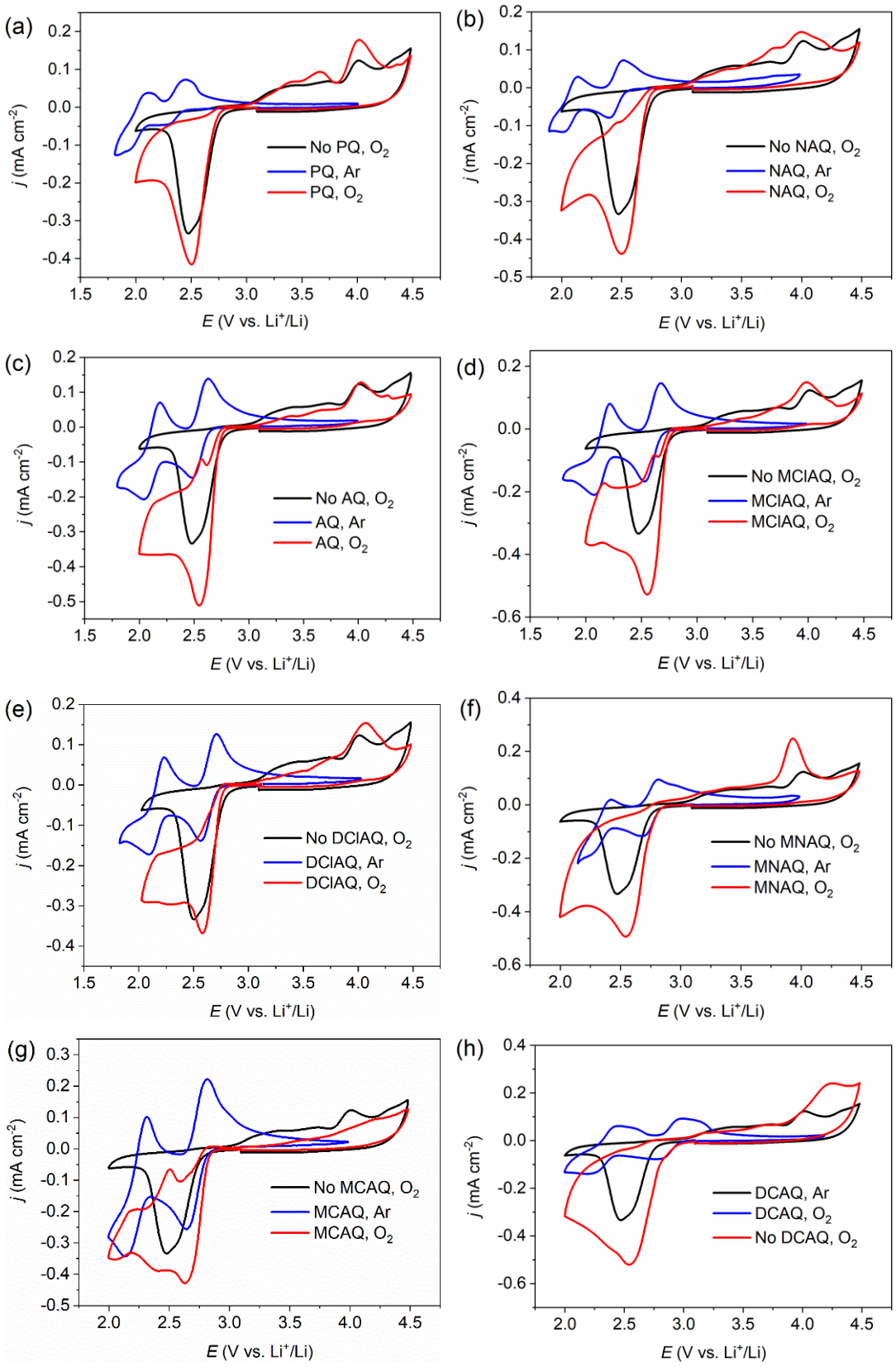
(a)
No PQ, O2
PQ, Ar
PQ, O2
(b)
No NAQ, O2
NAQ, Ar
NAQ, O2
(c)
No AQ, O2
AQ, Ar
AQ, O2
(d)
No MClAQ, O2
MClAQ, Ar
MClAQ, O2
(e)
No DClAQ, O2
DClAQ, Ar
DClAQ, O2
(f)
No MNAQ, O2
MNAQ, Ar
MNAQ, O2
(g)
No MCAQ, O2
MCAQ, Ar
MCAQ, O2
(h)
DCAQ, Ar
DCAQ, O2
No DCAQ, O2
j (mA cm-2)
E (V vs. Li+/Li)

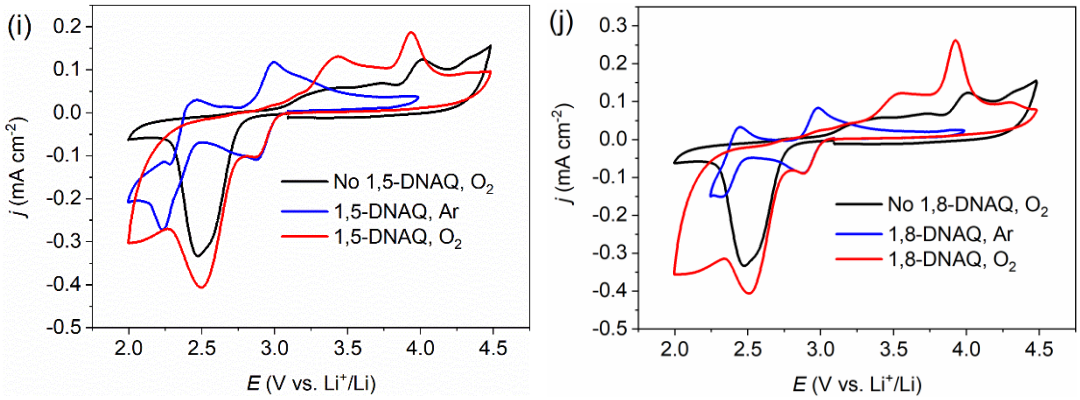

Fig. S11 Cyclic voltammograms of ten AQ-based compounds (2 mM) in 0.1 M $LiClO_4$-DMSO saturated by Ar (blue trace), O_2 (red trace). The black trace is a cyclic voltammogram observed in the base solution without ORRM. (a) PQ; (b) NAQ; (c) AQ; (d) MClAQ; (e) DClAQ ; (f) MNAQ; (g) MCAQ; (f) DCAQ; (i) 1,5-DNAQ; (j) 1,8-DNAQ. All CVs were observed on a gold electrode. The CV curves show different behavior of the electrochemical and chemical process for the same ORRM comparing with that in the tetraglyme based electrolyte.

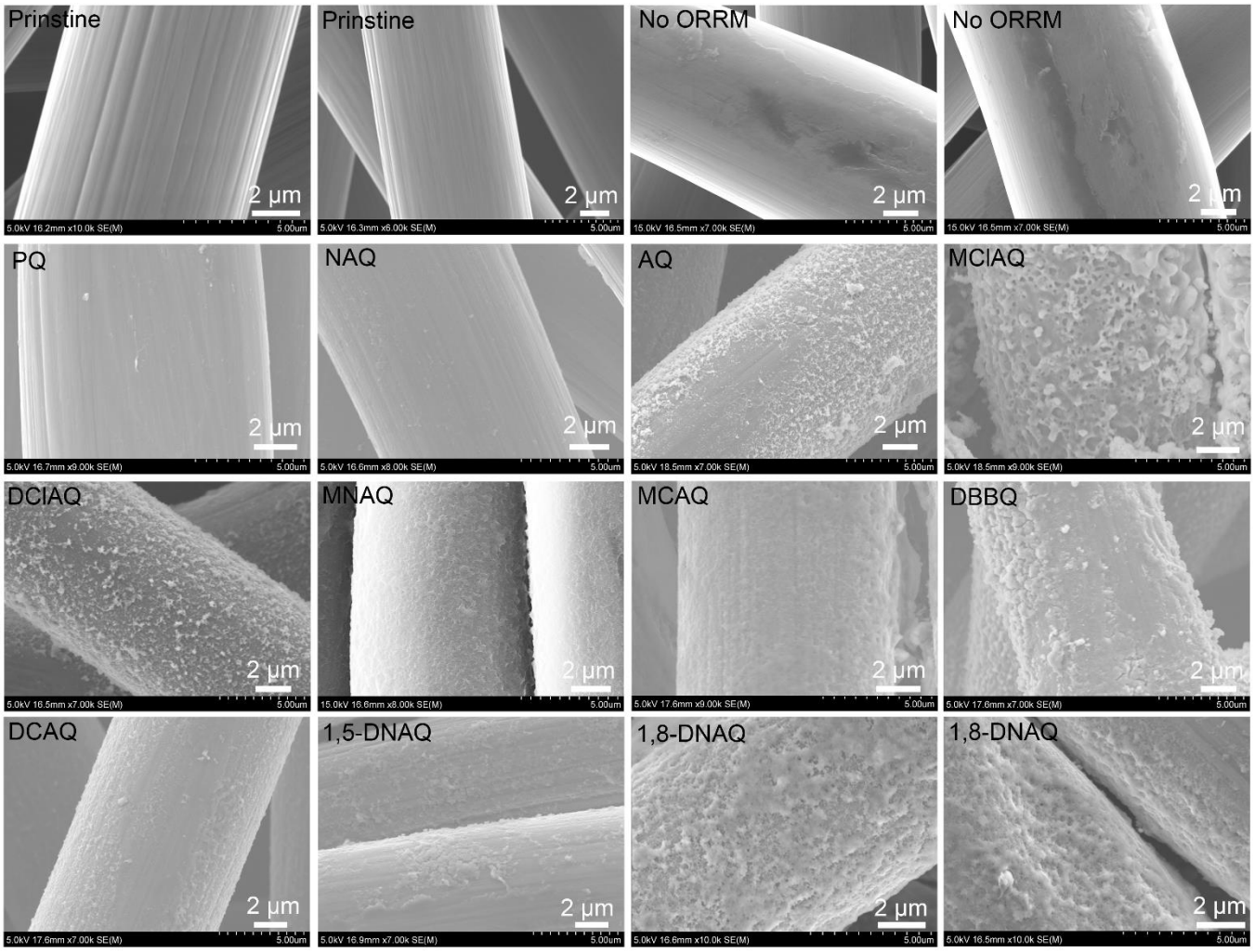

Fig.S12 SEM images of the pristine carbon electrode and discharged cathode with and without ORRMs in a low water content oxygen atmosphere (0.2 ppm) for all the tested ORRMs. Scale bar (2 μm), magnification, and the acceleration voltage are showed at the bottom of each figure with the name of the corresponding ORRM. Supplement for Fig. 6.

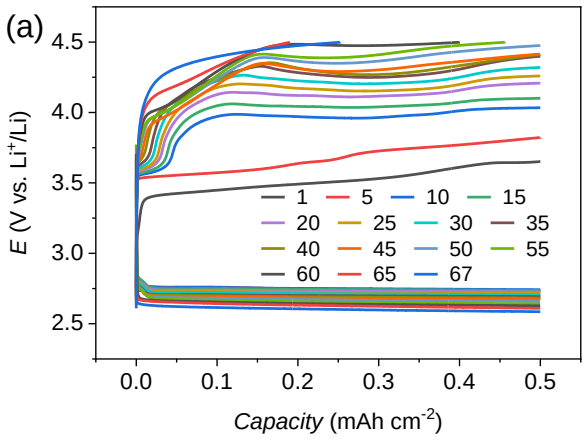

Fig. S13 The repeated discharge-charge behaviors observed in 0.5 M LiTFSI-TEGDME with ORRM (1,5-DNAQ, 10 mM suspension solution) and OERM (TEMPO, 30 mM) at a current density of 0.1 mA cm^{-2} under pure oxygen with the water content of 0.2 ppm The capacity was used as 0.5 mAh cm^{-2}. Li metal was used as the anode. In the cases of 1,8-DNAQ-TEMPO and DBBQ-TEMPO system, the cycle test failed due to the side reactions induced by Li metal.

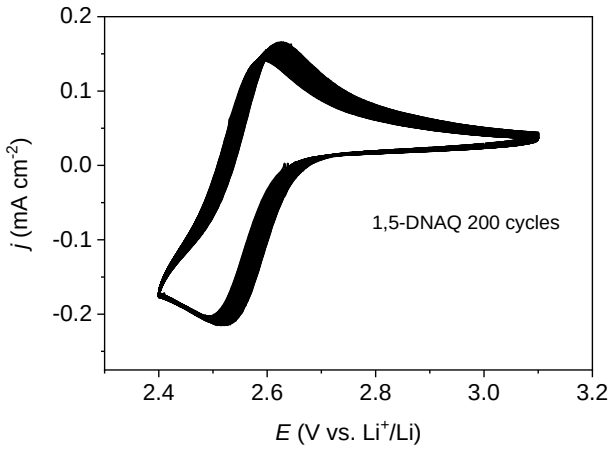

Fig. S14 200 cycles CV observed on a glassy carbon electrode in 0.5 M LiTFSI-TEGDME with 10 mM (suspension solution) 1,5-DNAQ. The scan rate is 50 mV s^{-1}. The volume of electrolyte in each CV test is 5 mL. The 1,5-DNAQ shows stable reversibility and stability in the measured potential range under Ar. The peak potential of 1,5-DNAQ has a little negative shift due to reaction between 1,5-DNAQ and Li-induced potential shift because the passive layer on the Li metal was destroyed when it was wrapped on the nickel wire as counter and reference.

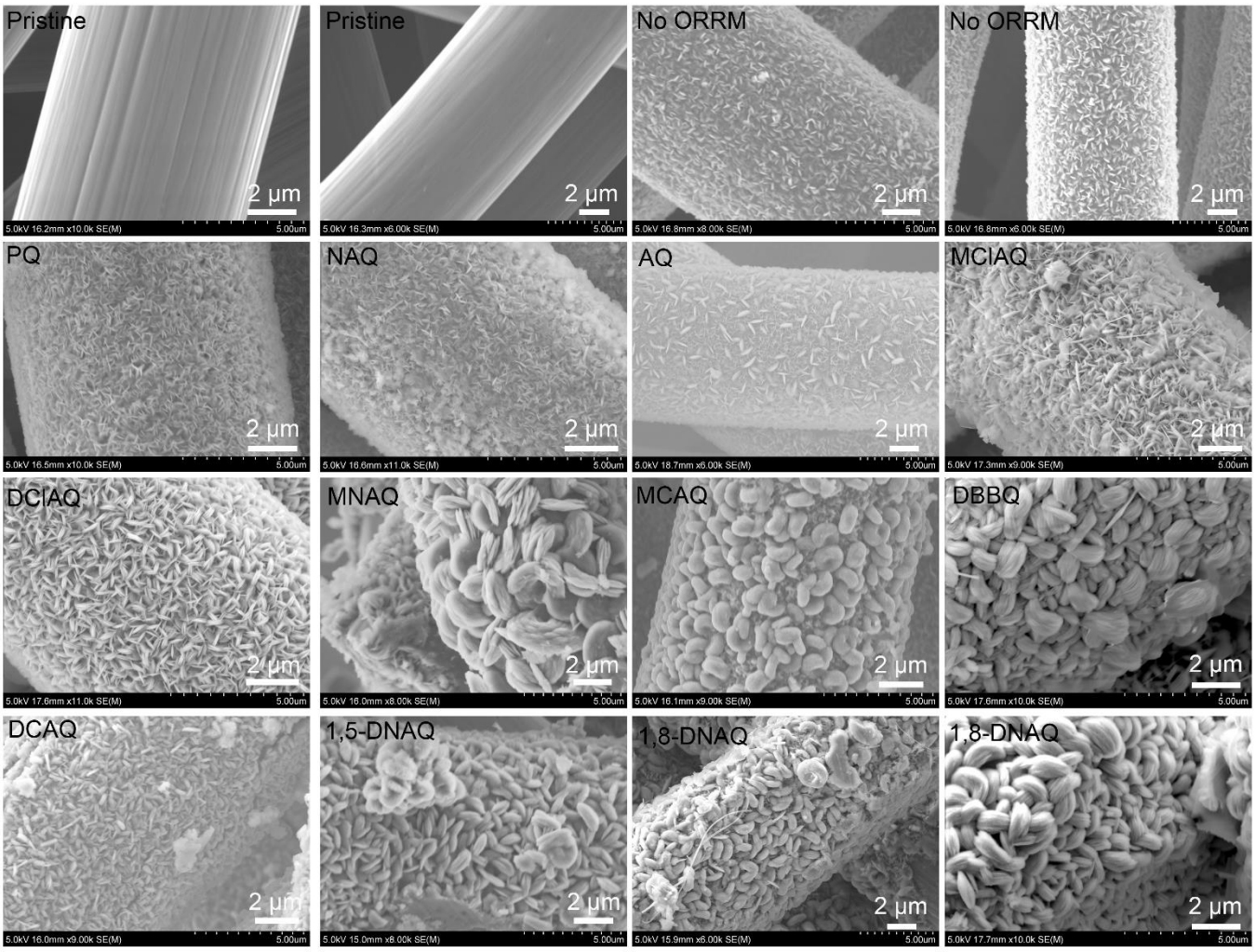

Fig. S15 SEM images of the pristine carbon electrode and discharged cathode with and without ORRMs in a high water content oxygen atmosphere (RH 5%). Scale bar (2 μm) under each image, magnification, and the acceleration voltage are showed at the bottom of each figure with the name of the corresponding ORRM. Supplement for Fig. 9.

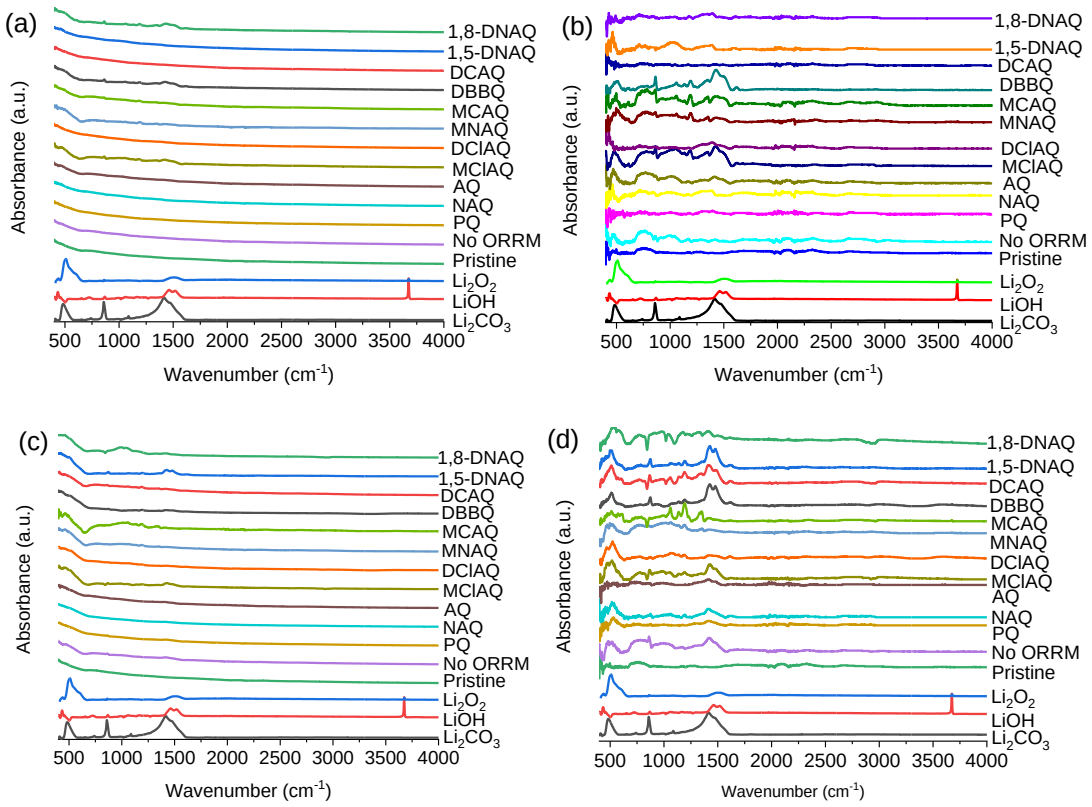

Fig. S16 ATR-IR spectroscopy of discharge cathode under (a,b) low water content and (c, d) high water content, (a, c)raw data, and (b, d) baseline correction.

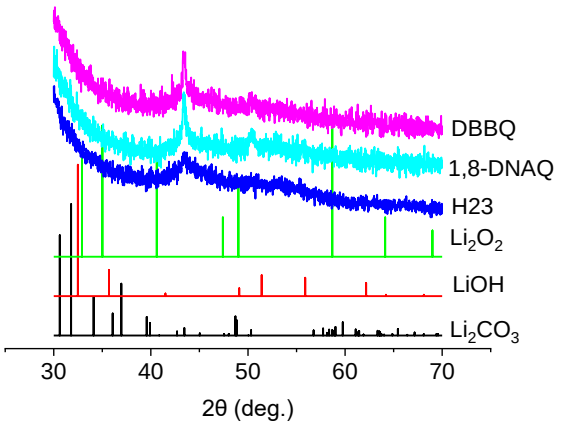

Fig. S17 The XRD results of the cathode discharged with 1,8-DNAQ and DBBQ under low water content oxygen (0.2 ppm). No signals for discharge products or sida products were observed except for those from the carbon paper (H23).

Reference

1. Schwenke, K. U.; Meini, S.; Wu, X.; Gasteiger, H. A.; Piana, M., Stability of superoxide radicals in glyme solvents for non-aqueous Li-O_2 battery electrolytes. *Phys Chem Chem Phys* **2013,** *15*, 11830-11839.

2. Gao, X.; Chen, Y.; Johnson, L.; Bruce, P. G., Promoting solution phase discharge in Li-O_2 batteries containing weakly solvating electrolyte solutions. *Nat Mater* **2016,** *15*, 882-888.

3. Hartmann, P.; Bender, C. L.; Sann, J.; Durr, A. K.; Jansen, M.; Janek, J.; Adelhelm, P., A comprehensive study on the cell chemistry of the sodium superoxide (NaO_2) battery. *Phys Chem Chem Phys* **2013,** *15*, 11661-11672.

4. O'Sullivan, D. W.; Tyree, M., The kinetics of complex formation between Ti(IV) and hydrogen peroxide. *International Journal of Chemical Kinetics* **2007,** *39*, 457-461.